Carbohydrate Polymers 98 (2013) 161–167

Contents lists available at SciVerse ScienceDirect

Carbohydrate Polymers

journal homepage: www.elsevier.com/locate/carbpol

# Preparation and characterization of bionanocomposite fiber based on cellulose and nano-$SiO_2$ using ionic liquid

Hong-Zan Song*, Zhi-Qiang Luo, Chun-Zheng Wang, Xue-Fang Hao, Jun-Gang Gao

*College of Chemistry & Environmental Science, Hebei University, Baoding 071002, PR China*

ARTICLE INFO

*Article history:*
Received 25 October 2012
Received in revised form 13 May 2013
Accepted 28 May 2013
Available online 5 June 2013

*Keywords:*
Cellulose
Ionic liquid
Nano-$SiO_2$
Bionanocomposite
Rheology

ABSTRACT

Microcrystalline cellulose (MCC)/nano-$SiO_2$ composite fibers were processed from solutions in 1-allyl-3-methylimidazolium chloride (AMIMCl) by the method of dry-jet wet spinning. The oscillatory shear measurements demonstrated that the gel network formed above 10 wt% nano-$SiO_2$ and the complex viscosity increased with increasing nano-$SiO_2$. Remarkably, the shear viscosity of the nanofluids was even lower than solutions without nano-$SiO_2$ under high shear rates. Scanning electron microscopy (SEM) and transmission electron microscopy (TEM) images revealed that well-dispersed particles exhibit strong interfacial interactions with cellulose matrix. Measurements on wide-angle X-ray diffraction (WAXD) indicated that the regenerated cellulose and nanocomposite fibers were the typical cellulose II crystalline form, which was different from the native cellulose with the polymorph of Type I. The tensile strength of the nanocomposite fibers was larger than that of pure cellulose fiber and showed a tendency to increase and then decrease with increasing nano-$SiO_2$. Furthermore, the nanocomposite fibers exhibited improved thermal stability.



## 1. Introduction

Cellulose, as the most plentiful and renewable resource in nature, is amongst the most widely used natural fibers (Chen et al., 2006; Hirano, Usutani, Yoshikawa, & Midorikawa, 1998; Kadokawa, Murakami, Takegawa, & Kaneko, 2009; Klemm, Heublein, Fink, & Bohn, 2005; Kosan, Michels, & Meister, 2008). However, cellulose is difficult to process in solution or as a melt, because of its large proportion of intra- and intermolecular hydrogen bonds, which strictly limit its processing and applications (Cai & Zhang, 2006; Ruan, Zhang, Zhou, Jin, & Chen, 2004). Therefore, many organic and inorganic solvent systems such as *N*-methyl morpholine *N*-oxide (NMMO) (Fink, Weigel, Purz, & Ganster, 2001), lithium chloride/1,3-dimethyl-2-imidazolidinone (LiCl/DMI) (Takaragi, Minoda, Miyamoto, Liu, & Zhang, 1999), lithium chloride/N, N-dimethylacetamide (LiCl/DMAc) (McCormick and Callais, 1987; McCormick, Callais, & Hutchinson, 1985), and phosphoric acid (Northolt et al., 2001) have been investigated for regenerated cellulose fiber production. Nevertheless, most of the systems still seem to be unsuccessful from an industrial viewpoint because of their toxicity and difficult solvent recovery. Recently, ionic liquids (ILs), which are considered as desirable green solvents, have been reported to be effective and promising cellulose solvents (Rinaldi, 2011; Song et al., 2013; Swatloski, Spear, Holbrey, & Rogers, 2002; Zhang, Wu, Zhang, & He, 2005; Zhu et al., 2006). Nowadays, ILs used for manufacturing-regenerated cellulose fibers are arousing considerable commercial interest because of their superior dissolving capacity, environmentally friendly properties, easy recycling and good recoverability (Rahatekar et al., 2009; Xu et al., 2008; Zhang et al., 2007).

Polymer nanocomposites with nanoparticles, such as organic and inorganic nanoparticals, have attracted much attention owing to their outstanding mechanical, optical, electrical (Kim, Abdala, & Macosko, 2010; Sahoo, Rana, Cho, Li, & Chan, 2010; Zhang et al., 2007), and flame retardancy properties (Dong et al., 2012; Kiliaris and Papaspyrides, 2010; Zhang, Yang, Maurer, & F, 2011; Zou, Wu, & Shen, 2008). Of these polymer nanocomposites, cellulose combined with natural polymers led to the development of a new class of biodegradable and environmental friendly bionanocomposites (Jia, Li, Ma, Sun, & Zhu, 2012; Siqueira, Bras, & Dufresne, 2010; Valodkar and Thakore, 2011). This new family of nanocomposites is expected to have remarkable improvement of material properties when compared with the matrix polymers, and it will capture new market in transportation, medical and packaging applications (Celis, Adelino, Hermosín, & Cornejo, 2012; Darder, Aranda, & Ruiz-Hitzky, 2007). However, the main challenges still exist for developing high-performance cellulose nanocomposites is how to improve the dispersion of nanoparticles in the cellulose matrix or solutions, which is of great use for modifying the physical properties of cellulose (Maniruzzaman, Jang, & Kim, 2012; Park, Liang,

* Corresponding author. Tel.: +86 312 5079369; fax: +86 312 5079359.
*E-mail address:* shzhbu@hbu.edu.cn (H.-Z. Song).

0144-8617/$ – see front matter © 2013 Elsevier Ltd. All rights reserved.
http://dx.doi.org/10.1016/j.carbpol.2013.05.079

Mohanty, Misra, & Drzal, 2004). Interestingly, ILs has been exploited as key components of dispersion medium in some novel systems, such as surfactant solutions, block copolymer micelle solutions, and emulsions (Anderson, Pino, Hagberg, Sheares, & Armstrong, 2003; Greaves and Drummond, 2008; He, Li, Simone, & Lodge, 2006). Specifically, because ILs can exhibit strong interactions with some nanopatarticles, a number of novel systems with ILs have recently been reported with respect to the dispersion of solid nanoparticles (Dupont and Scholten, 2010; Fukushima et al., 2006; Wang, Chu, & Li, 2008; Wu et al., 2009). Of these solid nanoparticles, nano-$SiO_2$ is widely used with ILs as nanohybrid solid-state electrolytes (Shimano, Zhou, & Honma, 2007), ionogels (Bideau, Viau, & Vioux, 2011; Moganty et al., 2012), and other advaced soft materials (Ueno and Watanabe, 2011; Wang, Zakeeruddin, Comte, Exnar, & Grätzel, 2003). In addition, nano-$SiO_2$ can easily provide functionalities by using ILs (Trewyn, Whitman, & Lin, 2004). Therefore, the use of ILs can not only as a solvent but also as a dispersion medium for preparing of cellulose nanocomposites.

In our previous work, the phase transitions and rheological properties of cellulose/AMIMCl and cellulose/1-ethyl-3-methylimidazolium acetate (EMIMAc) solutions under both oscillatory and steady shear modes were further studied (Song, Zhang, Niu, & Wang, 2010; Song, Niu, Wang, & Zhang, 2011). For cellulose/nano-$SiO_2$/AMIMCl solutions, however, situations might be quite different due to nanoparticles drastically alter the viscoelastic properties of the system (Rahatekar et al., 2009; Ueno, Hata, Katakabe, Kondoh, & Watanabe, 2008). In the present work, we reported the rheology and a facile and economic method for preparing bionanocomposite fibers based on cellulose and nano-$SiO_2$ with IL, as well as a detailed study of structure and properties of the resulting bionanocomposites fibers. It should be noted that IL appears to play a dual role as a solvent of cellulose and a dispersion medium of nanoparticles.

## 2. Materials and methods

### 2.1. Materials

The ionic liquid of 1-allyl-3-methylimidazolium chloride (AMIMCl) was synthesized according to the procedure described in the literature. Purification of AMIMCl was carried out on the basis of our previous work (Song et al., 2010). The water content of AMIMCl measured by the Karl Fischer titration was 0.12 wt%. Microcrystalline cellulose (MCC), Vivapur 101, used in this study was purchased from the Sen-Jun Chemical Agents Accessories Co., Ltd., Shanghai, China. The viscosity-average degree of polymerization (DP) of MCC in cupriethylenediamin hydroxide solution is about 200 as measured by using Ubbelodh viscometer. The nano-$SiO_2$ used in this study, NYSi80, was purchased from BOYU GAOKE New Material Co., Ltd., Beijing, China. The primary particles of the NYSi80 are 80 nm in diameter and have hydrophilic silanol (Si—OH) groups on their surface. The silica particles were dried for 24 h in a vacuum oven at 60 °C before use.

### 2.2. Composites preparation

Cellulose/nano-$SiO_2$/AMIMCl solutions were prepared as follows: Six batches of 5 g MCC were added into 89.8, 89.7, 89.6, 89.5, and 89.4 g AMIMCl in six sealed reaction vessels, respectively, and the mixtures were stirred at 90 °C for 4 h to obtain a homogeneous solution. Meanwhile, six batches of 0.2, 0.3, 0.4, 0.5, and 0.6 g nano-$SiO_2$ were dispersed in 5 g AMIMCl using mortar and pestle for 1 h to obtain a homogenous paste mixture, respectively, then, the obtained nano-$SiO_2$/AMIMCl paste mixtures were correspondingly added into the above six sealed reaction vessels and stirred for another 1 h at 90 °C until solutions were optically homogenous. Finally, 5 wt% MCC/AMIMCl solutions containing 0.2, 0.3, 0.4, 0.5, and 0.6 wt% were obtained with a total weight of 100 g, respectively. The method of preparing 7 and 9 wt% cellulose/nano-$SiO_2$/AMIMCl solutions samples were the same as above. Correspondingly, these solutions were used to prepare regenerated MCC/nano-$SiO_2$ (4, 6, 8, 10, and 12 wt%) composite fibers in the following section. The water content in each solution measured by the Karl Fischer titration was about 0.15 wt%. Before further measurements, the solutions were sealed and stored in desiccators containing $P_2O_5$.

Cellulose/nano-$SiO_2$ composite fibers were processed using dry-jet wet spinning with 3 cm air-gap and using deionized water as coagulation bath. For all samples, a single-hole spinneret of 200 μm was used. The fiber was first soaked in deionized water overnight and then washed with deionized water at least five times to remove AMIMCl. After, the fibers had been dried in vacuum at 80 °C for 48 h.

### 2.3. Rheological measurements

Rheological properties of the MCC/Nano-$SiO_2$/AMIMCl solutions under both oscillatory and steady shear modes were measured by using a TA AR2000ex stress-controlled rheometer with 25 mm and 40 mm parallel-plates geometry. The chosen gap was about 600 μm for all the measurements. Steady shear measurements and dynamic frequency sweep measurements were carried out within the shear rate range of 0.01–100 $s^{-1}$ and frequency range of 0.1–100 rad/s, respectively. Before the oscillatory shear measurements, a strain sweep from 0.1 to 100% with a fixed frequency of 6.28 rad/s was performed for each solution to determine the linear viscoelastic regime. The selected strain of 10–15% during the frequency sweeps fell well into the linear viscoelastic regime. The experimental temperature was mainly set at 30 °C. All measurements were conducted under a nitrogen atmosphere. In our experiments, the samples of 5 wt% and 7 wt% cellulose/nano-$SiO_2$/AMIMCl solutions were performed using 40 mm parallel plate geometry, while the samples of 9 wt% cellulose/nano-$SiO_2$/AMIMCl solutions were performed using 25 mm parallel plate geometry. To ensure data accuracy and repeatability, three measurements were carried out for each sample.

### 2.4. Scanning electron microscopy (SEM)

The observation of composite fiber samples was taken on a JEOL SEM 6700 microscope operating at 5 kV. The fibers were frozen in liquid nitrogen, immediately fractured, and vacuum-dried. The fracture surface of the fibers was coated with platinum layer (the thick is about 20 nm) before the observation.

### 2.5. Transmission electron microscopy (TEM)

The ultrathin slices with a thickness of approximately 70–90 nm were obtained from composite fiber samples imbedded into an epoxy resin by ultra-microtome (Leica EM UC6 & FC6) under cryogenic conditions, and then it was placed onto a carbon-coated copper grid. The dispersion state of Nano-$SiO_2$ within cellulose was investigated by using a JEOL JEM-2200 FS at an accelerating voltage of 200 kV.

### 2.6. Wide-angle X-ray diffraction (WAXD)

WAXD profiles of MCC and MCC/nano-$SiO_2$ composite fibers were obtained by using an X-ray diffractometer (D/MAX-2500, Rigaku Denki, Japan) with Cu Kα radiation ($\lambda = 0.154$ nm) at 40 kV and 100 mA. The samples were scanned continuously from $2\theta = 5°$ to 40° at a rate of 1°/min and the WAXD profiles were recorded at an interval of 0.02°.

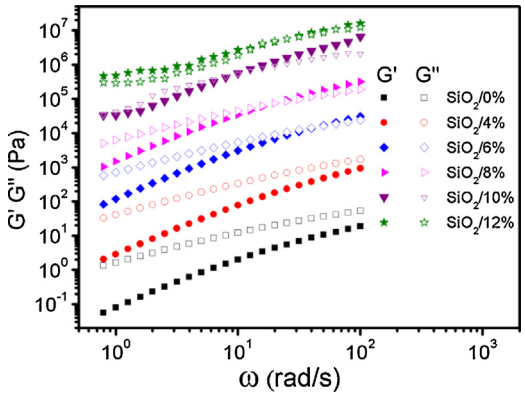


**Fig. 1.** Changes of storage ($G'$) and loss ($G''$) moduli as a function of angular frequency for 7% MCC/AMIMCl solution with different content of nano-$SiO_2$ at 30 °C. The data are shifted along the vertical axis by multiplying $10^n$ with corresponding $n$ values of −2, −1, 0, 1, and 2, respectively, to prevent data overlap.

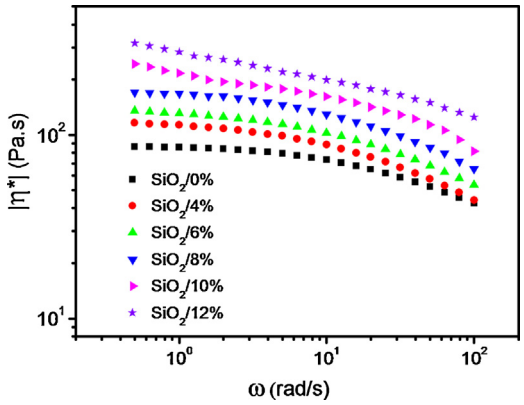


**Fig. 2.** Changes of complex viscosity as a function of angular frequency for the 7% MCC/AMIMCl solutions with different content of nano-$SiO_2$ at 30 °C.

### 2.7. Mechanical performance

The tensile testing of the single regenerated MCC/nano-$SiO_2$ composite fibers (diameter 15–20 μm with length of 50 mm) was measured by using a universal testing machine (Instron 1122, UK) at a crosshead speed of 5 mm/min; a gauge length of 30 mm was used. Fiber ends were glued onto a paper frame according to the preparation procedure described in ASTM D3822-07 Standard (Andersons, Poriķe, & Spārniņš, 2009; Mukhopadhyay, Fangueiro, Arpaç, & Şentürk, 2008). Mechanical tests were performed at room temperature. To ensure data accuracy and repeatability, at least five measurements were carried out for each composite fiber.

### 2.8. Thermogravimetric (TGA)

The decomposition behaviors of the fibers were measured on the Perkin-Elmer Pyris 6 type thermogravimetric analyzer (TGA) in the temperature range of 50–500 °C under nitrogen atmosphere at the heating rate of 20 °C/min. The fibers were rolled into small balls (between 1.5 mg and 2 mg) by hand (wearing latex gloves to avoid moisture transfer), and then placed on the sample pan. To ensure data accuracy and repeatability, three measurements were carried out for each composite fiber.

## 3. Results and discussion

### 3.1. Rheological properties of cellulose/IL solutions with different content of nano-$SiO_2$

In general, small amounts of nanoparticles drastically alter the viscoelastic properties of the material (Du et al., 2004; Rahatekar et al., 2009; Wang, Wang, Lou, & Hao, 2010). In our current study, both the oscillatory and steady shear measurements were first performed for the MCC/nano-$SiO_2$/AMIMCl solutions system. The changes of storage ($G'$) and loss ($G''$) moduli as a function of angular frequency ($\omega$) for 7 wt% MCC/AMIMCl solutions with different content of nano-$SiO_2$ at 30 °C are shown in Fig. 1. The plots are shifted along the vertical axis by multiplying $10^n$ with corresponding $n$ values of −2, −1, 0, 1 and 2, respectively, to prevent data overlap. The nano-$SiO_2$ content (with respect to the weight of the cellulose) ranges from 4 to 12 wt% as indicated. For the solutions with nano-$SiO_2$ content below 6 wt%, $G'$ scales approximately with $\omega$ by $G'$–$\omega^2$ and $G''$–$\omega$ at low frequencies; moreover, $G'$ is always smaller than $G''$ and no crossover is found within the detected frequency range, which indicates that these solutions exhibit a liquid-like behavior. The terminal cross-over point is related with the entanglement degree and the longest relaxation time ($\tau_d$), time of cellulose chains diffusing out of the original tube. As the nano-$SiO_2$ content increases from 6 to 10 wt%, a crossover of $G'$ and $G''$ appears, and the frequency of the cross-over point, $\omega_x$, moves evidently to lower values with increasing nano-$SiO_2$ concentration, indicating the longest relaxation time ($\tau_d \propto 1/\omega_x$) increases with the increase of nano-$SiO_2$ content. In addition, $G'$ and $G''$ of the solution (10 *wt%*) shows a deviation from the terminal slope of 2 and 1 at low frequencies, respectively. For the solution of nano-$SiO_2$ content 12 wt%, $G''$ is less than $G'$ over the whole frequency range, and the values of $G''$ and $G'$ are nearly independent of frequency, which indicates a typical gel-like behavior (Roy, Budtova, & Navard, 2003; Weng, Zhang, Ruan, Shi, & Xu, 2004; Ruan, Lue, & Zhang, 2008). This gel-like behavior is attributed to the formation of network structure caused by strong interactions among cellulose chains, nano-$SiO_2$ and ionic liquids (Chang, Hung, Chang, Jiang, & Lin, 2011).

Fig. 2 shows the changes of complex viscosity, $|\eta^*|$, as a function of angular frequency for the 7 wt% MCC/AMIMCl solutions with different nano-$SiO_2$ at 30 °C. When the cellulose concentration is below 10 wt%, $|\eta^*|$ values show proportional increase with increasing nano-$SiO_2$ content. At the low nano-$SiO_2$ content (4 and 8 wt%), the solutions basically show the Newtonian plateau region in the low frequency range and shear-thinning behavior is observed in the high frequency range. Whereas for the high nano-$SiO_2$ content solutions (10 wt%), another shear-thinning behavior is observed in the low frequency range and the width of Newtonian plateau region decreases. Whereas the Newtonian plateau region disappears and $|\eta^*|$ shows almost linear decrease with increasing frequency when the nano-$SiO_2$ content exceeds 10 wt%, which suggests an existence of gelating network. This can be also attributed to the fact that the physical junctions in the solutions are strengthened with increasing nano-$SiO_2$ content.

Fig. 3 shows the changes of viscosity as a function of shear rate for the 7 wt% MCC/AMIMCl solutions with different nano-$SiO_2$ content at 30 °C. It can be seen that for the solution with the low nano-$SiO_2$ content, i.e. 6 wt%, a Newtonian plateau appears at the low shear rates and one shear-thinning region appears at the high shear rates, which is similar to that of conventional polymeric fluids. With increasing nano-$SiO_2$ content (10–12 wt%), the shear thinning property in a wide shear rate range shows a distinctly non-Newtonian behavior, indicating the transient network is formed through interactions among cellulose chains, nano-$SiO_2$ and ionic liquids. Moreover, it also exhibits slight shear thickening at low shear rates while shear thinning above a critical shear rate, being highly viscous but also elastic due to the existence of a stably transient network. Such shear-thinning behavior derived from the shear-induced disruption of interparticle physical bonds that can be observed in many of the typical dispersions of colloidal

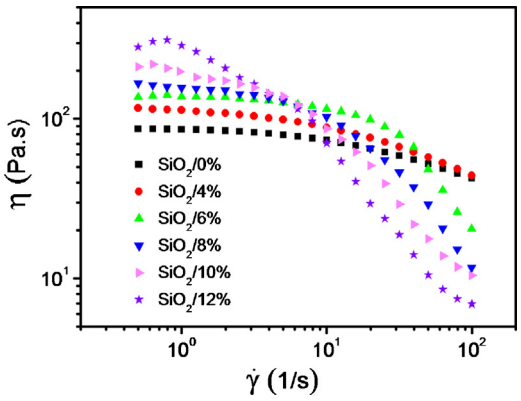


**Fig. 3.** Steady shear flow curves for the 7% MCC/AMIMCl solutions with different content of nano-$SiO_2$ at 30 °C.

particles. Furthermore, the shear viscosity of these solutions with nano-$SiO_2$ (6–12 wt%) is lower than the viscosity of MCC/AMIMCl solution without nano-$SiO_2$ at much higher shear rate.

### 3.2. Structural and morphology of cellulose nanocomposite fibers

Regenerated cellulose and cellulose/nano-$SiO_2$ composite fibers with nano-$SiO_2$ content of 4, 6, 8, 10, and 12 wt% were fabricated by dry-jet wet-spinning. Both the cellulose and cellulose/nano-$SiO_2$ composite fibers with a smooth surface of side surface sections were seen in Fig. 4a and b, indicating the dry-jet wet-spinning process allowed the facile fabrication of cellulose nanocomposite fibers.

Fig. 5a–d shows SEM images of the cross sections for cellulose and cellulose/nano-$SiO_2$ composite fibers containing 8 wt% nano-$SiO_2$. In Fig. 5a and b, the cross sections surface of cellulose fiber is generally flat and featureless. The similar morphology was observed for cellulose fiber from NaOH/thiourea aqueous solution. This suggests that the behavior cellulose fiber is brittle and the crack propagates in a planar manner. However, for cellulose/nano-$SiO_2$ composite fiber (Fig. 5c and d), the cross section surface was extremely rough. This is clearly distinctive, compared to the flat fracture surface of cellulose fiber as shown in Fig. 5a, indicating the addition of nano-$SiO_2$ will improve the mechanical properties of cellulose, such as tensile strength and toughness. In Fig. 5d, in higher magnification, the embedded filler particles also exhibit good interfacial bonding with cellulose (as shown by black arrow). Moreover, the void like feature created by distortional pullout silica particles is also observed (as shown by white arrow), suggesting strong interface adherence between cellulose and nano-$SiO_2$. Therefore, it can be deduced that the mechanical properties of the composites will profit from the strong interface adherence. We also used TEM to observe the dispersion of nano-$SiO_2$ within the cellulose matrix (Fig. 5e). The TEM observation shows that the nano-$SiO_2$ was well-dispersed and the size was about 80 nm in diameter.

It is known that cellulose I and II are the most studied forms of cellulose, and cellulose II has higher chemical reactivity than cellulose I and can be made into excellent cellulosic materials, so it is regarded as one of the most useful biomaterials and has broad applications in chemical industry. Moreover, the crystal structure and crystallinity of cellulose also depends on the additives, leading to the change in mechanical properties and thermal stability (Han, Yan, Chen, Li, & Bangal, 2011; Wang et al., 2010). The structures of cellulose nanocomposite fiber were further examined by using WAXD technique. Fig. 6 shows WAXD patterns of original cellulose powder, regenerated cellulose fiber, and cellulose nanocomposite fiber containing 8 wt% nano-$SiO_2$. It can be seen that the original cellulose powder exhibits three obvious crystalline peaks at 14.9°, 16.2° and 22.5°, which are characteristics of the cellulose I family. The diffraction pattern of regenerated cellulose fiber shows a broad profile containing two weak crystalline peaks appearing at 20.0° and 21.6°, corresponding to the (1 1 0) and (2 0 0) planes, respectively, as also observed for viscose rayon, cuprammonium rayon and the celluloses regenerated by rapid coagulation from NaOH/Urea aqueous solution, which are attributed to the typical cellulose II crystalline form (Ruan et al., 2004). For regenerated cellulose fiber, two crystalline peaks appearing at 20.0° and 21.6° are also observed but the peak appearing at 20.0° becomes blunt and weak. Clearly, the nano-$SiO_2$ particles do not display any crystalline peaks, which is consistent with the silica nanoparticles being noncrystalline at that size scale.

### 3.3. Properties of cellulose nanocomposite fibers

It is well-known that one of the primary reasons for adding inorganic fillers to polymers is to improve their mechanical performance. Therefore, the mechanical properties of polymer nanocomposites are most concerned. Furthermore, tensile testing is the most widely used method to evaluate the mechanical properties of the resultant nanocomposites. The tensile strength of a material is the maximum amount of tensile stress that it can take before failure, for example breaking. For cellulose fibers, the tensile strength is the stress coordinate on the stress–strain curve at the point of rupture. The stress–strain curves are shown in Fig. 7. It can be seen that when the nano-$SiO_2$ content is less than 8 wt%, the tensile strength increases with increasing nano-$SiO_2$ content. At 8 wt% nano-$SiO_2$, fiber tensile strength increased by about 21%. However, when the nano-$SiO_2$ exceeds 8 wt%, the tensile strength decreases. On the other hand, with the addition of nano-$SiO_2$ from 0 to 6 wt%, the elongation at break of the fibers increases, while

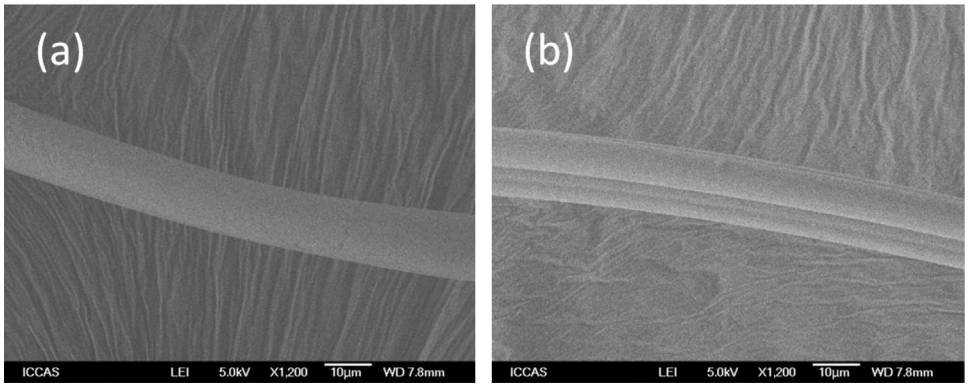


**Fig. 4.** SEM images of side surface sections of cellulose (a) and cellulose/nano-$SiO_2$ (b) fibers. The nano-$SiO_2$ content is 8 wt%.

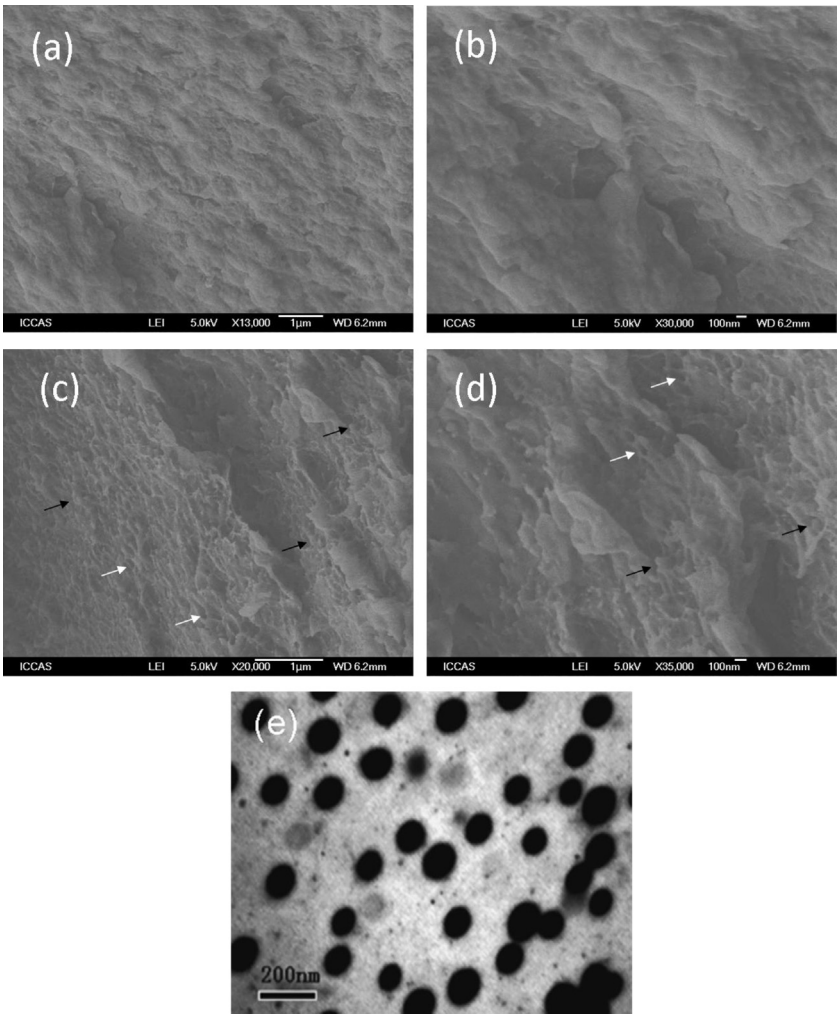


**Fig. 5.** SEM images of cross sections for cellulose fiber (a and b) and cellulose/nano-$SiO_2$ fiber (c and d). (b) and (d) are the magnified image of (a) and (c), respectively. A TEM image of the nanocomposite fiber (e). The nano-$SiO_2$ content is 8 wt%.

it decreases when the nano-$SiO_2$ exceeds 6 wt%. The similar phenomenon has been observed on PP/$SiO_2$ and PA6/$SiO_2$ composites, which due to the increased tendency of $SiO_2$ nanoparticles to form agglomerates at higher concentrations (Zou et al., 2008). Note that all the nanoreinforced fibers have larger tensile strength than pure cellulose fiber, which due to the strong interaction between cellulose and nano-$SiO_2$ (Portugal, Dias, Duarte, & Evtuguin, 2010).

TGA is the most popular method for characterizing the thermal stability of polymers and polymer composites. Fig. 8 shows the effect of nano-$SiO_2$ on thermal stability of cellulose fibers. The temperature of maximum weight loss rate ($T_{max}$) obtained from DTG curve is taken as the characteristic temperature of the degradation process. Apparently, the nanocomposites exhibit higher thermal

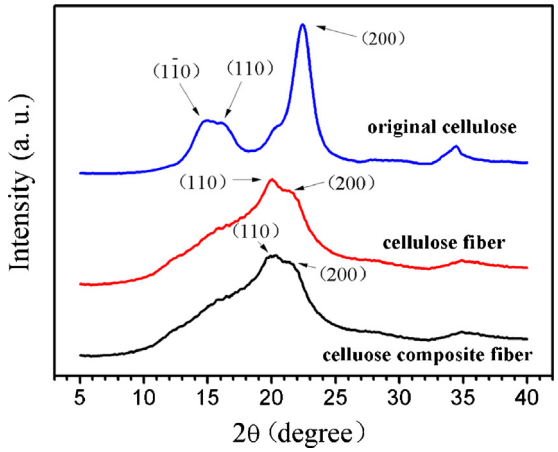


**Fig. 6.** WAXD patterns of original cellulose powder, regenerated cellulose fiber, and cellulose nanocomposite fibers containing 8 wt% nano-$SiO_2$.

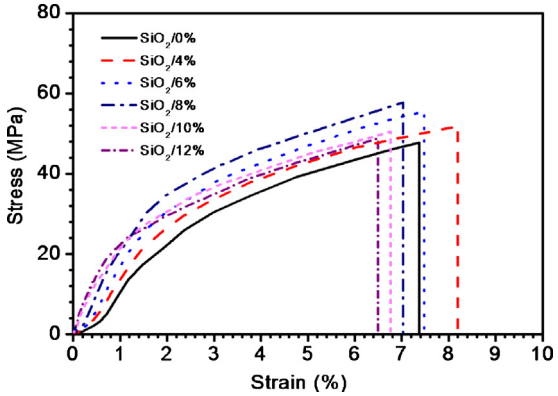


**Fig. 7.** Stress–strain curves of regenerated MCC/nano-$SiO_2$ composite fibers with different content of nano-$SiO_2$.

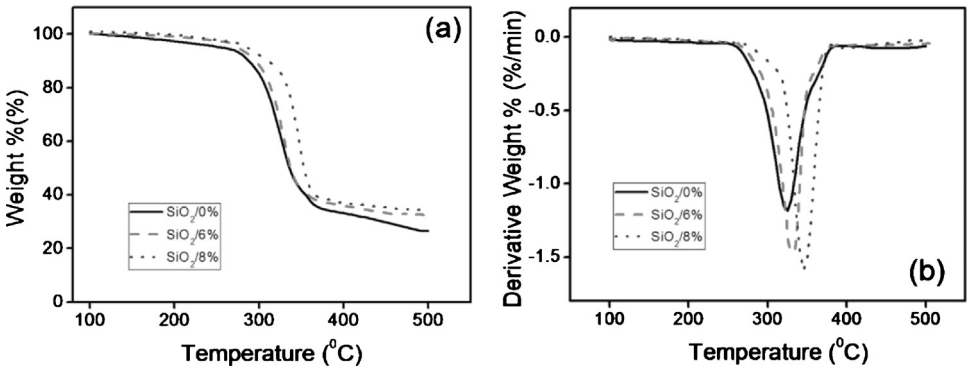


**Fig. 8.** Thermal gravimetric (TG) (a) and differential thermal gravimetric (DTG) (b) curves for different cellulose nanocomposite fibers.

stability and the $T_{max}$ increases with increasing nano-$SiO_2$ content. For the nanocomposite fiber containing 8 wt% nano-$SiO_2$, the $T_{max}$ is 345.4 °C, which is 22.1 °C higher than in the case of the pure cellulose fiber (323.3 °C). It can also be seen from TG curve that the residues increased by almost the same amount as the amount of nano-$SiO_2$ incorporated into the cellulose. This means that the loss of nano-$SiO_2$ in coagulation bath is very little during spinning.

## 4. Conclusions

In this paper, bionanocomposite fibers based on cellulose and nano-$SiO_2$ were prepared by the method of dry-jet wet spinning using an ionic liquid, AMIMCl as a good solvent for cellulose and well dispersant for nanoparticles. From the oscillatory shear measurements it was found that the storage moduli ($G'$) and viscosity of the solution became larger with the increase of nano-$SiO_2$ content, and the gelating network was found to occur above 10 wt% nano-$SiO_2$. Remarkably, the shear viscosity of the solutions with nano-$SiO_2$ was even lower than that of cellulose/IL solutions under high shear rates. Well-dispersed particles were observed in cellulose nanocomposite fibers. Furthermore, the cross section surface of cellulose fiber was flat, whereas the composite fiber was extremely rough. The regenerated cellulose and nanocomposite fibers were the typical cellulose II crystalline form, which was totally different from the native cellulose with the dominated polymorph of Type I. The tensile strength of the nanocomposite fibers was larger than that of pure cellulose fiber and showed a tendency to increase and then decrease with increasing nano-$SiO_2$ content and has maximum values at 8 wt% nano-$SiO_2$ content. The nanocomposites exhibited higher thermal stability and the $T_{max}$ increased with increasing nano-$SiO_2$ content. In addition, the residues increased by almost the same amount as the amount of nano-$SiO_2$ incorporated into the cellulose, which means that the loss of nano-$SiO_2$ in coagulation bath is very little during spinning. Therefore, this work provides a potential application in the field of bionacomposite fiber manufacturing.

## Acknowledgements

HZ Song acknowledges the financial supports from the Specialized Research Fund for the Doctoral Program of Higher Education (Grant No. 20121301120004), the Natural Science Foundation of Hebei Province (Grant No. B2013201117), the Plan of Science Technology Research and Development of Hebei Province (Grant No. 12211204), Hebei University (Grant No. Y2011223) and Baoding Bureau of Science and Technology (Grant No. 12ZG023).

## References

Anderson, J. L., Pino, V., Hagberg, E. C., Sheares, V. V., & Armstrong, D. W. (2003). Surfactant solvation effects and micelle formation in ionic liquids. *Chemical Communications*, *19*, 2444–2445.

Andersons, J., Porike, E., & Spārniņš, E. (2009). The effect of mechanical defects on the strength distribution of elementary flax fibres. *Composites Science and Technology*, *69*, 2152–2157.

Bideau, J. L., Viau, L., & Vioux, A. (2011). Ionogels, ionic liquid based hybrid materials. *Chemical Society Reviews*, *40*, 907–925.

Cai, J., & Zhang, L. N. (2006). Unique gelation behavior of cellulose in NaOH/Urea aqueous solution. *Biomacromolecules*, *7*, 183–189.

Celis, R., Adelino, M. A., Hermosín, M. C., & Cornejo, J. (2012). Montmorillonite–chitosan bionanocomposites as adsorbents of the herbicide clopyralid in aqueous solution and soil/water suspensions. *Journal of Hazardous Materials*, *209–210*, 67–76.

Chang, H. C., Hung, T. C., Chang, S. C., Jiang, J. C., & Lin, S. H. (2011). Interactions of silica nanoparticles and ionic liquids probed by high pressure vibrational spectroscopy. *Journal of Physical Chemistry C*, *115*, 11962–11967.

Chen, X. M., Burger, C., Fang, D. F., Ruan, D., Zhang, L. N., Hsiao, B. S., et al. (2006). X-ray studies of regenerated cellulose fibers wet spun from cotton linter pulp in NaOH/thiourea aqueous solutions. *Polymer*, *47*, 2839–2848.

Darder, M., Aranda, P., & Ruiz-Hitzky, E. (2007). Bionanocomposites: A new concept of ecological, bioinspired, and functional hybrid materials. *Advanced Materials*, *19*, 1309–1319.

Dong, Q. X., Ding, Y. Fen, Wen, B., Wang, F., Dong, H. C., Zhang, S. M., et al. (2012). Improvement of thermal stability of polypropylene using DOPO-immobilized silica nanoparticles. *Colloid and Polymer Science*, *290*, 1371–1380.

Du, F. M., Scogna, R. C., Zhou, W., Brand, S., Fischer, J. E., & Winey, K. I. (2004). Nanotube networks in polymer nanocomposites: Rheology and electrical conductivity. *Macromolecules*, *37*, 9048–9055.

Dupont, J., & Scholten, J. D. (2010). On the structural and surface properties of transition-metal nanoparticles in ionic liquids. *Chemical Society Reviews*, *39*, 1780–1804.

Fink, H., Weigel, P., Purz, H. J., & Ganster, J. (2001). Structure formation of regenerated cellulose materials from NMMO-solutions. *Progress in Polymer Science*, *26*, 1473–1524.

Fukushima, T., Kosaka, A., Yamamoto, Y., Aimiya, T., Notazawa, S., Takigawa, T., et al. (2006). Dramatic effect of dispersed carbon nanotubes on the mechanical and electroconductive properties of polymers derived from ionic liquids. *Small*, *2*, 554–560.

Greaves, T. L., & Drummond, C. J. (2008). Ionic liquids as amphiphile self-assembly media. *Chemical Society Reviews*, *37*, 1709–1726.

Han, D. L., Yan, L. F., Chen, W. F., Li, W., & Bangal, P. R. (2011). Cellulose/graphite oxide composite films with improved mechanical properties over a wide range of temperature. *Carbohydrate Polymers*, *83*, 966–972.

He, Y. Y., Li, Z. B., Simone, P., & Lodge, T. P. (2006). Self-assembly of block copolymer micelles in an ionic liquid. *Journal of the American Chemical Society*, *128*, 2745–2750.

Hirano, S., Usutani, A., Yoshikawa, M., & Midorikawa, T. (1998). Fiber preparation of *N*-acylchitosan and its cellulose blend by spinning their aqueous xanthate solutions. *Carbohydrate Polymers*, *37*, 311–313.

Jia, N., Li, S. M., Ma, M. G., Sun, R. C., & Zhu, J. F. (2012). Hydrothermal fabrication, characterization, and biological activity of cellulose/$CaCO_3$ bionanocomposites. *Carbohydrate Polymers*, *88*, 179–184.

Kadokawa, J. I., Murakami, M. A., Takegawa, A., & Kaneko, Y. (2009). Preparation of cellulose-starch composite gel and fibrous material from a mixture of the polysaccharides in ionic liquid. *Carbohydrate Polymers*, *75*, 180–183.

Kiliaris, P., & Papaspyrides, C. D. (2010). Polymer/layered silicate (clay) nanocomposites: An overview of flame retardancy. *Progress in Polymer Science*, *35*, 902–958.

Kim, H., Abdala, A. A., & Macosko, C. W. (2010). Graphene/polymer nanocomposites. *Macromolecules*, *43*, 6515–6530.

Klemm, D., Heublein, B., Fink, H. P., & Bohn, A. (2005). Cellulose: Fascinating biopolymer and sustainable raw material. *Angewandte Chemie-International Edition*, *44*, 3358–3393.

Kosan, B., Michels, C., & Meister, F. (2008). Dissolution and forming of cellulose with ionic liquids. *Cellulose*, *15*, 59–66.

Maniruzzaman, M., Jang, S. D., & Kim, J. (2012). Titanium dioxide-cellulose hybrid nanocomposite and its glucose biosensor application. *Materials Science and Engineering: B*, *117*, 844–848.

McCormick, C. L., & Callais, P. A. (1987). Derivatization of cellulose in lithium chloride and N-N-dimethylacetamide solutions. *Polymer*, *28*, 2317–2323.

McCormick, C. L., Callais, P. A., & Hutchinson, B. H., Jr. (1985). Solution studies of cellulose in lithium chloride and N,N-dimethylacetamide. *Macromolecules*, *18*, 2394–2401.

Moganty, S. S., Srivastava, S., Lu, Y. Y., Schaefer, J. L., Rizvi, S. A., & Archer, L. A. (2012). Ionic liquid-tethered nanoparticle suspensions: A novel class of ionogels. *Chemistry of Materials*, *24*, 1386–1392, 2012.

Mukhopadhyay, S., Fangueiro, R., Arpaç, Y., & Şentürk, Ü. (2008). Banana fibers-variability and fracture behaviour. *Journal of engineered fibers and fabrics*, *3*, 39–45.

Northolt, M. G., Boerstoel, H., Maatman, H., Huisman, R., Veurink, J., & Elzerman, H. (2001). The structure and properties of cellulose fibres spun from an anisortopic phosphoric acid solution. *Polymer*, *42*, 8249–8264.

Park, H. M., Liang, X. M., Mohanty, A. K., Misra, M., & Drzal, T. L. (2004). Effect of compatibilizer on nanostructure of the biodegradable cellulose acetate/organoclay nanocomposites. *Macromolecules*, *37*, 9076–9082.

Portugal, I., Dias, V. M., Duarte, R. F., & Evtuguin, D. V. (2010). Hydration of cellulose/silica hybrids assessed by sorption isotherms. *Journal of Physical Chemistry B*, *114*, 4047–4055.

Rahatekar, S. S., Rasheed, A., Jain, R., Zammarano, M., Koziol, K. K., Windle, A. H., et al. (2009). Solution spinning of cellulose carbon nanotube composites using room temperature ionic liquids. *Polymer*, *50*, 4577–4583.

Rinaldi, R. (2011). Instantaneous dissolution of cellulose in organic electrolyte solutions. *Chemical Communications*, *47*, 511–513.

Roy, C., Budtova, T., & Navard, P. (2003). Rheological properties and gelation of aqueous cellulose-NaOH solutions. *Biomacromolecules*, *4*, 259–264.

Ruan, D., Lue, A., & Zhang, L. N. (2008). Gelation behaviors of cellulose solution dissolved in aqueous NaOH/thiourea at low temperature. *Polymer*, *49*, 1027–1036.

Ruan, D., Zhang, L. N., Zhou, J. P., Jin, H. M., & Chen, H. (2004). Structure and properties of novel fibers spun from cellulose in NaOH/thiourea aqueous solution. *Macromolecular Bioscience*, *4*, 1105–1112.

Sahoo, N. G., Rana, S., Cho, J. W., Li, L., & Chan, S. H. (2010). Polymer nanocomposites based on functionalized carbon nanotubes. *Progress in Polymer Science*, *35*, 837–867.

Shimano, S., Zhou, H. S., & Honma, I. (2007). Preparation of nanohybrid solid-state electrolytes with liquid like mobilities by solidifying ionic liquids with silica particles. *Chemistry of Materials*, *19*, 5216–5221.

Siqueira, G., Bras, J., & Dufresne, A. (2010). Cellulosic bionanocomposites: A review of preparation, properties and applications. *Polymers*, *2*, 728–765.

Song, H. Z., Niu, Y. H., Wang, Z. G., & Zhang, J. (2011). Liquid crystalline transition and gel–sol transitions for concentrated microcrystalline cellulose (MCC)/1-ethyl-3-methylimidazolium acetate (EMIMAc) solutions. *Biomacromolecules*, *12*, 1087–1096.

Song, H. Z., Niu, Y. H., Yu, J., Zhang, J., Wang, Z. G., & He, J. S. (2013). Preparation and morphology of different types of cellulose spherulites from concentrated cellulose ionic liquid solutions. *Soft Matter*, *9*, 3013–3020.

Song, H. Z., Zhang, J., Niu, Y. H., & Wang, Z. G. (2010). Phase transition and rheological behaviors of concentrated cellulose/ionic liquid solutions. *Journal of Physical Chemistry B*, *114*, 6006–6013.

Swatloski, R. P., Spear, S. K., Holbrey, J. D., & Rogers, R. D. (2002). Dissolution of cellulose with ionic liquids. *Journal of the American Chemical Society*, *124*, 4974–4975.

Takaragi, A., Minoda, M., Miyamoto, T., Liu, H., & Zhang, L. N. (1999). Reaction characteristics of cellulose in the LiCl/1,3-dimethyl-2-imidazolidinone solvent system. *Cellulose*, *6*, 93–102.

Trewyn, B. G., Whitman, C. M., & Lin, V. S. Y. (2004). Morphological control of room-temperature ionic liquid templated mesoporous silica nanoparticles for controlled release of antibacterial agents. *Nano Letters*, *4*, 2139–2143.

Ueno, K., Hata, K., Katakabe, T., Kondoh, M., & Watanabe, M. (2008). Nanocomposite ion gels based on silica nanoparticles and an ionic liquid: Ionic transport, viscoelastic properties, and microstructure. *Journal of Physical Chemistry B*, *112*, 9013–9019.

Ueno, K., & Watanabe, M. (2011). From colloidal stability in ionic liquids to advanced soft materials using unique media. *Langmuir*, *27*, 9105–9115.

Valodkar, M., & Thakore, S. (2011). Organically modified nanosized starch derivatives as excellent reinforcing agents for bionanocomposites. *Carbohydrate Polymers*, *86*, 1244–1251.

Wu, B. H., Hu, D., Kuang, Y. J., Liu, B., Zhang, X. H., & Chen, J. H. (2009). Functionalization of carbon nanotubes by an ionic-liquid polymer: Dispersion of Pt and PtRu nanoparticles on carbon nanotubes and their electrocatalytic oxidation of methanol. *Angewandte Chemie-International Edition*, *48*, 4751–4754.

Wang, B. G., Wang, X. B., Lou, W. J., & Hao, J. C. (2010). Rheological and tribological properties of ionic liquid-based nanofluids containing functionalized multi-walled carbon nanotubes. *Journal of Physical Chemistry C*, *114*, 8749–8754.

Wang, J. Y., Chu, H. B., & Li, Y. (2008). Why single-walled carbon nanotubes can be dispersed in imidazolium-based ionic liquids. *ACS Nano*, *2*, 2540–2546.

Wang, P., Zakeeruddin, S. M., Comte, P., Exnar, I., & Grätzel, M. (2003). Gelation of ionic liquid-based electrolytes with silica nanoparticles for quasi-solid-state dye-sensitized solar cells. *Journal of the American Chemical Society*, *125*, 1166–1167.

Weng, L. H., Zhang, L. N., Ruan, D., Shi, L. H., & Xu, J. (2004). Thermal gelation of cellulose in a NaOH/thiourea aqueous solution. *Langmuir*, *20*, 2086–2093.

Xu, S. S., Zhang, J., He, A. H., Li, J. X., Zhang, H., & Han, C. C. (2008). Electrospinning of native cellulose from nonvolatile solvent system. *Polymer*, *49*, 2911–2919.

Zhang, H., Wang, Z. G., Zhang, Z. N., Wu, J., Zhang, J., & He, J. S. (2007). Regenerated-cellulose/multiwalled-carbon-nanotube composite fibers with enhanced mechanical properties prepared with the ionic liquid 1-allyl-3-methylimidazolium chloride. *Advanced Materials*, *19*, 698–704.

Zhang, H., Wu, J., Zhang, J., & He, J. S. (2005). 1-Allyl-3-methylimidazolium chloride room temperature ionic liquid: A new and powerful nonderivatizing solvent for cellulose. *Macromolecules*, *38*, 8272–8277.

Zhang, J. H., Yang, M. S., Maurer, H. J., & Frans. (2011). Effect of $TiO_2$ formation on the free volume properties of electrospun PMMA nanohybrids. *Macromolecules*, *44*, 5711–5721.

Zhu, S. D., Wu, Y. X., Chen, Q. M., Yu, Z. N., Wang, C. W., Jin, S. W., et al. (2006). Dissolution of cellulose with ionic liquids and its application: A mini-review. *Green Chemistry*, *8*, 325–327.

Zou, H., Wu, S. S., & Shen, J. (2008). Polymer/silica nanocomposites: Preparation, characterization, properties, and applications. *Chemical Reviews*, *108*, 3893–3957.